EEET ECOLOGICAL ENGINEERING & ENVIRONMENTAL TECHNOLOGY

Ecological Engineering & Environmental Technology, 2025, 26(4), 300–310
https://doi.org/10.12912/27197050/201328
ISSN 2719–7050, License CC-BY 4.0

Received: 2025.01.21
Accepted: 2025.02.22
Published: 2025.03.01

Methanolic leaf extract of *Indigofera tinctoria* mediated biosynthesis of zinc oxide nanoparticles

Arini Rajab[1,2], Abd. Wahid Wahab[1*], Paulina Taba[1], Syahruddin Kasim[1], Abdur Rahman Arif[1], Fatimah[3], M. Yasser[1,4]

[1] Department of Chemistry, Hasanuddin University, Makassar 90245, South Sulawesi, Indonesia
[2] Department of Environmental Pollution Control Engineering Technology, Samarinda State Polytechnic of Agriculture, Samarinda 75131, East Kalimantan, Indonesia
[3] Department of Medical Laboratory Technology, Stikes Panrita Husada, Bulukumba 92561, South Sulawesi, Indonesia
[4] Department of Chemical Engineering, State Polytechnic of Ujung Pandang, Makassar 90245, South Sulawesi, Indonesia
* Corresponding author's email: wahidwahab@unhas.ac.id

ABSTRACT

Zinc oxide (ZnO) nanoparticles are multifunctional materials with wide application potential. The aim of this research is to synthesize ZnO nanoparticles utilizing *Indigofera tinctoria* leaf extract in methanol as an eco-friendly reducing and stabilizing agent. Synthesis was carried out with variations in extract mass, namely 1 g (Z1), 5 g (Z5), and 10 g (Z10) to evaluate the effect of the extract concentration upon the characteristics of the nanoparticles. FTIR, XRD, SEM, XRF, and UV-Vis DRS were used to characterize the samples. FTIR analysis results showed typical ZnO peaks at wave numbers 422-430 cm^{-1}. XRD analysis revealed that the nanoparticles have a hexagonal wurtzite crystal structure with space group P63mc. The crystallite size decreased as the extract concentration increased, amounting to 16.55 nm (Z1), 15.21 nm (Z5), and 13.75 nm (Z10). The band gap energy value increased from 3.19 eV (Z1) to 3.21 eV (Z10), indicating an increase in optical activity at higher extract concentrations. Morphological analysis by SEM showed that all samples exhibited a quasi-spherical shape. EDS characterization revealed that only Zn and O elements were identified. XRF results confirmed the pristineness of ZnO nanoparticles, with a ZnO content of 98.99%. This research provides new insights into the potential use of *Indigofera tinctoria* leaf extract in the synthesis of ZnO nanoparticles, which can be utilized in various functional material and technology applications. These results also open up opportunities for the development of green synthesis methods for the fabrication of nanomaterials with characteristics that can be customized according to application needs.

Keywords: methanolic extract, *Indigofera tinctoria*, biosynthesis, ZnO, nanoparticles.

INTRODUCTION

Nanotechnology is a method and technique of treating materials to obtain materials with new functionalities and improve their characteristics (Lusvardi et al., 2017), and it can be applicable in many fields when combined with other research areas (Abbas et al., 2019). Nanotechnology has drawn the curiosity of researchers because it produces materials with good mechanical, electromagnetic, and optical properties (Chandrakala et al., 2022). Among various materials, nanoparticles play a special role in various applications. Nowadays, the desire for an environmentally friendly approach has led to the widespread implementation of green synthesis routes for producing metal oxide nanoparticles (Marouzi et al., 2021). The biosynthesis method is similar to the bottom-up approach in the chemical reduction process (Nabi et al., 2021).

Generally, leaf extracts are widely used in the metal oxides biosynthesis because leaves

are rich in metabolite compounds (Nadeem et al., 2018). Biosynthesis can be affected by the concentration of the plant extract. The quantity of plant extract can influence the size and shape of the nanoparticles (Ashour et al., 2023). Silver and gold nanoparticles have been synthesized using the aqueous leaf extract of *Indigofera tinctoria*. The presence phytochemicals in the leaf extract of *Indigofera tinctoria* have an influence on the production of nanoparticles (Vijayan et al., 2018). *Indigofera tinctoria* is a shrub in Fabaceae family. It is well-known as a medicinal plant (N et al., 2020) and has antimicrobial activity (Srinivasan et al., 2015). Studies showed that *Indigofera tinctoria* contains indigo color and applicable in dye-sensitized solar cell (DSSC) (Rajan & Cindrella, 2019).

ZnO nanoparticles are one of the most widely produced and used nanomaterials (Shaikhaldein et al., 2021). According to the US Food and Drug Administration (FDA), ZnO is known as a generally recognized as safe (GRAS) material (Rafeeq et al., 2021). As an n-type semiconductor, ZnO has an exciton binding energy of 60 meV and a band gap energy of 3.37 eV (Fu & Fu, 2015). ZnO is also known to be a good photocatalyst due to its good electrical and optical properties, non-toxic, inexpensive, and high photocatalytic activity (Sheik Mydeen et al., 2020). The biosynthesis that has been carried out using *Mimosa tenuiflora* extract shows that ZnO nanoparticles have the ability to degrade methyl orange, with yields reaching 96% in 90 minutes under UV irradiation and 62% for 180 minutes under sunlight (Quevedo-Robles et al., 2022). The methanolic leaf extract was employed in synthesis due to its excellent ability as a capping agent in nanoparticles production (Kumara Swamy et al., 2015). Moreover, previous report has shown that ZnO nanoparticles synthesized using methanol extract produce a smaller nanoparticle compared to aqueous extract (Mushtaq et al., 2023). Although the biosynthesis of ZnO nanoparticles using plant extracts has been widely carried out, most studies still focus on aqueous extracts of various plants. The use of methanolic extracts in the synthesis of ZnO nanoparticles is relatively rarely reported, although it is known that methanol has a better ability to extract phytochemical compounds than water. Therefore, this study investigates the biosynthesis of ZnO nanoparticles using methanolic leaf extract of *Indigofera tinctoria*, as well as evaluates the effect of varying extract concentration on the obtained nanoparticles.

MATERIALS AND METHODS

Materials

Fresh leaves of *Indigofera tinctoria* were collected at the local area in Kajang, Bulukumba, Indonesia. The chemicals used in this work, including natrium hydroxide (NaOH), methanol (CH_3OH), and zinc acetate dihydrate ($Zn(CH_3COO)_2 \cdot 2H_2O$), were ordered from Merck with no further purification.

Extract preparation

The fresh leaves were cleaned and air-dried. The dried leaves were then grounded. Methanol was added to 100 g of dried leaf and extracted for 45 minutes at 50 °C. The extraction procedure was accomplished using ultrasound-assisted extraction (Yasser et al., 2020). The extract was concentrated using a rotary vacuum evaporator.

Gas chromatography-mass spectroscopy analysis

GC-MS analysis was performed using GCMS-QP2010 Plus (Shimadzu). Rtx-5MS was used as column with length of 30.0 m, thickness of 0.25 μm, and diameter of 0.25 mm. The carrier gas used in the analysis was helium, which had 99.99% purity level. The chemical substances were identified by matching their spectra to the database.

Biosynthesis of ZnO nanoparticles

In this study we utilized methanolic leaf extract of *Indigofera tinctoria* as bioreductor in biosynthesis process. The nanoparticle fabrication was accomplished based on the previous study (Abomuti et al., 2021), with modifications. ZnO nanoparticles were synthesized with different leaf extract masses (1, 5, and 10 g) and labelled Z1, Z5, and Z10. The leaf extract was dissolved with double-distilled water (50 mL) in the beaker glass. After 10 minutes of stirring, the mixture was filtered. Zinc salt (5 g) was added to the mixture and stirred for 2 hours at 50 °C. Later on, NaOH 2M was added until the mixture attained pH 12 and then filtered after the next 2 hours. The

nanoparticles were dried for 8 hours at 60 °C. The obtained ZnO nanoparticles were calcined for 2 hours at 400 °C. Figure 1 illustrates the biosynthetic procedure.

Characterization of ZnO nanoparticles

Fourier transform infrared spectroscopy

FTIR analysis was performed using IRPrestige-21 Shimadzu. ZnO nanoparticles were mixed with KBr crystals then subjected to infrared scanning.

X-Ray diffraction

The crystal structure was determined using Shimadzu XRD-7000 with Cu-Kα radiation, between 15°–75°, scan speed 2.00 deg/min. The Scherrer formula was used to calculate the crystallite size (Adam et al., 2021) (Eq. 1).

$$D = \frac{K\lambda}{\beta \cos\theta} \quad (1)$$

where: λ is the X-ray wavelength, β is the full width at half maximum (FWHM), θ is the diffraction angle and k is a constant.

Scanning electron microscope-energy dispersive X-Ray spectroscopy

The morphology of ZnO nanoparticles was examined utilizing SEM, Hitachi SU3500, accelerating voltage 10kV and maximum magnification 100k. The elemental composition was examined using EDAX TEAM.

X-ray fluorescence

Thermofisher ARL QUANT'X EDXRF was used to analyse the chemical composition of ZnO nanoparticle.

UV-Vis diffuse reflectance spectroscopy

The optical characteristics were determined using UV-Vis DRS, Thermo Evolution 220 with scan speed 150 nm/min. The reflectance was measured at 200–800 nm.

RESULTS AND DISCUSSION

GC-MS analysis

The extract chromatogram is shown in Figure 2. The chromatographic peaks were obtained by GC-MS analysis from 3.5 to 42 min and thirteen compounds were identified. All the compounds have 90% and above similarity index according to database. The compounds with similarity index below 90% were not considered (Marín et al., 2018; Tahya & Karnelasatri, 2021). The compounds identified are presented in Table 1. The major component of the extract was identified at 14.864 min. The main component traced was mome inositol which is a polysaccharide. It has been reported that mome inositol can act as a bioreductor due to its capability in stabilizing and capping during biosynthesis (Joghee et al., 2019). Previous study

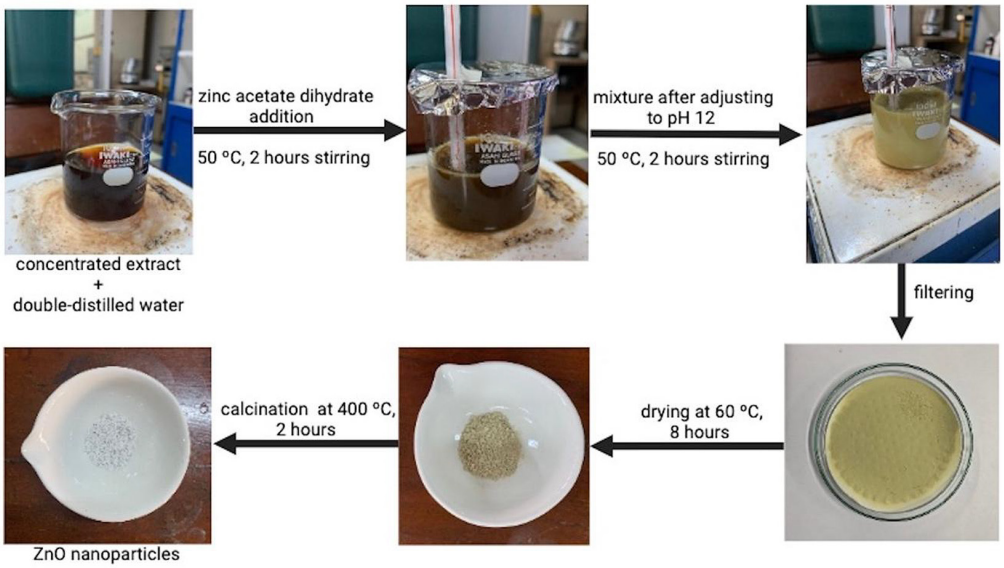

Figure 1. Schematic process of synthesizing ZnO nanoparticles

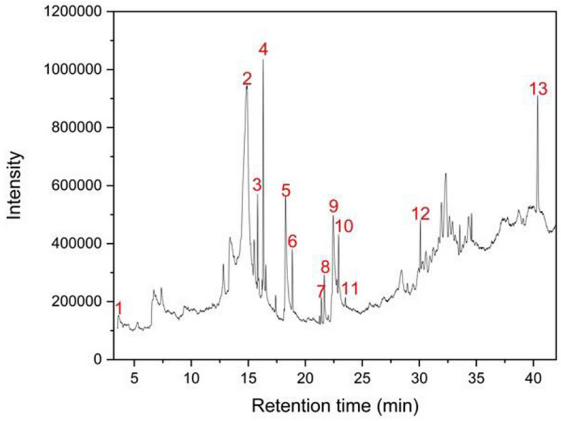

Figure 2. Methanolic leaf extract of *Indigofera tinctoria* chromatogram

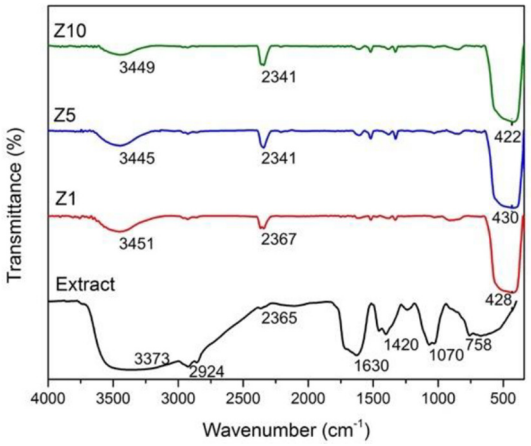

Figure 3. FTIR spectra of ZnO nanoparticles

reported that 26 compounds were detected in the extract of *Indigofera tincotria*.

FTIR analysis

The functional group of leaf extract and ZnO nanoparticles was examined within 4000–340cm^{-1}. The ZnO stretching vibration is associated with intense absorption peaks at 428 (Z1), 430 (Z5), and 422 cm^{-1} (Z10) in Figure 3. ZnO nanoparticles characteristic vibrations are identified by vibrational stretching at 400–600 cm^{-1} (Poonguzhali et al., 2021). A result comparable to the typical vibration peak at 422 cm^{-1} was observed in ZnO nanoparticles synthesized utilizing *Eucalyptus globulus* (Obeizi et al., 2020). The absorption at 2367 (Z1) and 2341 cm^{-1} (Z5 and Z10) were attributed to carbonyl stretching (Prasad & Joseph, 2024) due to the atmospheric CO_2 during analysis (Kaningini et al., 2022; Swamy et al., 2021). OH group vibrations marked by the broad and strong stretching at 3373 (extract), 3451 (Z1), 3445 (Z5), and 3449 cm^{-1} (Z10) (Alamdari et al., 2020; Sadiq et al., 2021), indicate flavonoids, saponins, and tannins (Fadhila et al., 2024). The FTIR spectrum of extract also showed absorption at 2924 cm^{-1} denoting C-H streching. A peak at 1630 cm^{-1} is linked to C=C vibration. The peak at 1402 cm^{-1} is typically associated wtih C-H bending vibration, at 1070 cm^{-1} could indicate C-O streching vibration, and peak at 758 cm^{-1} can be atributed to out-of-plane C-H bending vibration. FTIR spectra of ZnO nanoparticles displayed an absorption pattern that is comparable to the extract, albeit with a decreasing intensity. That indicates that plant biomolecules involved in biosynthesis surround ZnO nanoparticles, revealing

Table 1. GC-MS analysis of methanolic leaf extract of *Indigofera tinctoria*

No.	Retention time	Compounds
1.	3.641	1,2-cyclopentanedione
2.	14.864	Mome inositol
3.	15.845	Neophytadiene
4.	16.320	1,2-Benzenedicarboxylic acid, bis(2-methylpropyl) ester
5.	18.284	n-Hexadecanoic acid
6.	18.883	Hexadecanoic acid, ethyl ester
7.	21.421	9,12,15-Octadecatrienoic acid, methyl ester, (Z,Z,Z)-
8.	21.683	Phytol
9.	22.459	9,12,15-Octadecatrienoic acid, (Z,Z,Z)-
10.	22.928	(E)-9-Octadecenoic acid ethyl ester
11.	23.517	Octadecanoic acid, ethyl ester
12.	30.096	1,2-Benzenedicarboxylic acid
13.	40.385	Vitamin E

that biomolecules are crucial to the synthesis of nanoparticles (Dappula et al., 2023).

X-ray diffraction characterization

The diffractograms of Z1, Z5, and Z10 can be seen in Figure 4. No impurities associated with the diffraction peaks were detected. The peaks were allocated as (100), (002), (101), (012), (110), (013), (200), (112), (201), and (004) crystal planes. This result is in accordance with COD 96-900-4179. The pattern reveals that all the diffraction peaks indicate the typical peak of ZnO hexagonal wurtzite structure (Faisal et al., 2021; Nunes et al., 2024).

Table 2 displays that ZnO nanoparticles crystallite size is influenced by the different masses of extracts applied. As the concentration of the extract increases, the crystallite size of the prepared nanoparticles decreases (Parmar & Sanyal, 2022). ZnO nanoparticles crystallite size was 16.55 (Z1), 15.21 (Z5), and 13.75 nm (Z10). This finding is consistent with the prior study (Isnaeni et al., 2021) that the amount of the extract can control the nanoparticle crystallite size throughout the synthesis process. The crystallite size is smaller than the previously reported, which obtain crystallite size of ZnO nanoparticles produced utilizing aqueous leaf extract of *Indigofera tinctoria* was 22 nm (Chithiga & Manimegalai, 2023).

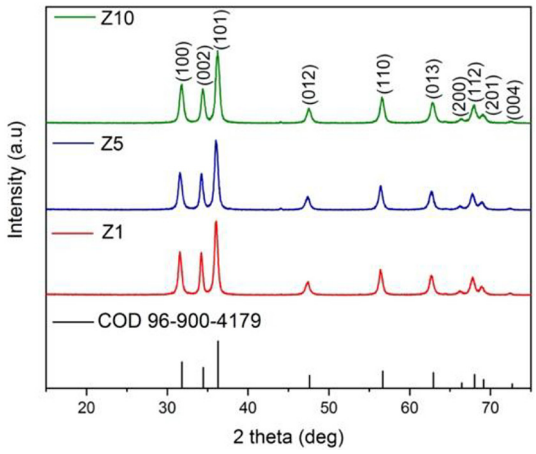

Figure 4. ZnO nanoparticles diffractogram

The Rietveld refinement technique was applied to ascertain the ZnO nanoparticle crystal structure using Rietica software (Rilda et al., 2022; Xie et al., 2024). Figure 5(a–c) illustrate the Rietveld refinement curves. The Rietveld refinement results verify that the synthesized nanoparticles represent a single phase. The crystal parameters after refinement are tabulated in Table 3. The reliability index, such as expected profile R-factor (R_{exp}), weight profile R-factor (R_{wp}), profile R-factor (R_p), and Chi-square (χ^2) show suitable values that confirm the accuracy of the refinement results (Ho et al., 2024). χ^2 values decline with the increase of the extract mass, which corroborated the successful refinement between experimental data and the theoretical plot (Geetha et al., 2016).

Morphological characterization

Figure 6(a-c) display the morphology of prepared ZnO nanoparticles at varying masses of leaf extract. The morphology of Z1, Z5, and Z10 was observed at 30.000× magnifications. The SEM images exhibit a quasi-spherical shape and

Table 2. ZnO nanoparticles crystallite size

hkl	Z1		Z5		Z10	
	2 theta (deg)	Crystallite size (nm)	2 theta (deg)	Crystallite size (nm)	2 theta (deg)	Crystallite size (nm)
100	31.58	16.36	31.60	15.04	31.78	14.22
002	34.22	19.85	34.24	17.50	34.42	15.28
101	36.06	16.99	36.08	16.01	36.24	15.05
012	47.38	13.97	47.38	13.20	47.56	13.22
110	56.42	16.52	56.42	15.91	56.60	14.64
013	62.70	15.58	62.70	14.34	62.86	13.92
200	66.22	12.07	66.22	11.05	66.40	8.45
112	67.80	14.71	67.78	14.07	67.92	13.30
201	68.92	16.82	68.94	15.37	69.10	12.95
004	72.42	22.62	72.44	19.63	72.60	16.45
	Average	16.55	Average	15.21	Average	13.75

Table 3. Refined parameters of prepared ZnO nanoparticles

Parameters	Z1	Z5	Z10
Space group	*P63mc*	*P63mc*	*P63mc*
a=b(Å)	3.2500	3.2482	3.2466
c(Å)	5.1999	5.2017	5.1998
V (Å^3)	47.5671	47.5305	47.4646
Z	2	2	2
α=β(°)	90	90	90
γ(°)	120	120	120
R_{exp}	19.49	20.49	19.53
R_{wp}	7.35	6.58	5.07
R_p	10.00	9.63	8.19
X^2	0.14	0.10	0.07

agglomerated. The morphology of Z1, Z5, and Z10 particles is similar to each other. The outcomes of the images are consistent with the prior reports, *Terminalia catappa* (Momoh et al., 2024) and *Agathosma betulina* (Thema et al., 2015) extract formed similar shaped ZnO nanoparticles. Figure 6(d-f) show the EDS spectra of Z1, Z5, and Z10. The spectra depict the elemental information of the products. The absence of other elements besides Zn and O in the spectra indicates the fabricated nanoparticles have high purity.

X-ray fluorescence characterization

The XRF analysis of Z10 is presented in Table 4, which contains 98.99% ZnO, while the proportions of CuO, P_2O_5, NiO, Nb_2O_5, and Rh_2O_3 were only in traces. It was revealed that the synthesized ZnO nanoparticles have negligible impurity (Nath et al., 2018). This finding aligns with the data from FTIR and XRD characterizations, validating the pristineness of the prepared nanoparticles in the present work.

Optical properties

Figure 7a illustrates that the absorption peaks for all samples are shown below 400 nm. The absorption peaks can be attributed to the intrinsic band-gap absorption of ZnO nanoparticles since the electron transitions from the valence band to the conduction band ($O_{2p} \rightarrow Zn_{3d}$) (Alshehri & Malik, 2019; Mthana et al., 2022). ZnO nanoparticles UV-Vis absorption occurs within 350–380 nm (Alyamani et al., 2021), which is specific to the wurtzite phase (Uribe-López et al., 2021). The reflectance spectra was analysed utilizing the Kubelka-Munk function (Eq. 2) (Ramesh et al., 2015).

Table 4. XRF analysis for Z10

Analytes	Composition %
ZnO	98.99
CuO	0.515
P_2O_5	0.236
NiO	0.197
Nb_2O_5	0.0426
Rh_2O_3	0.0053

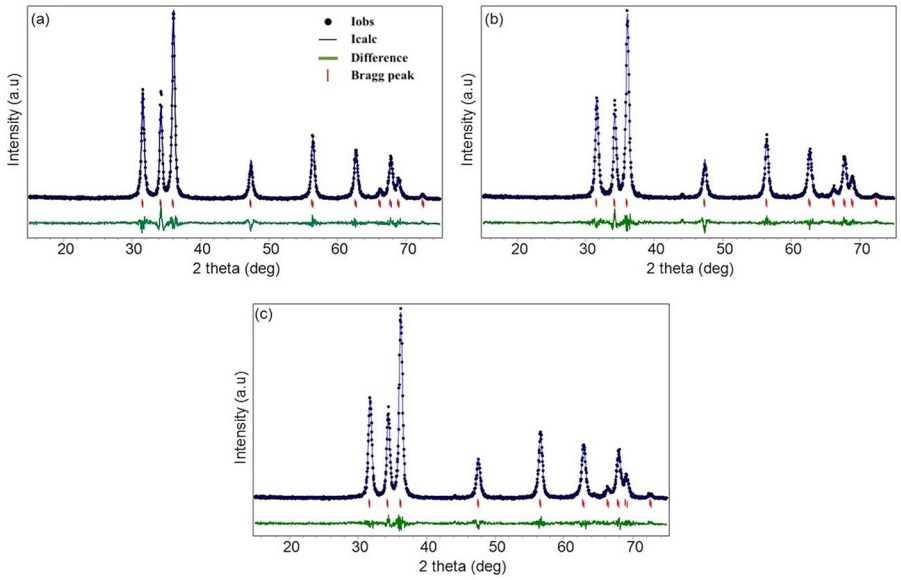

Figure 5. Rietveld refinement XRD patterns of Z1 (a), Z5 (b), and Z10 (c)

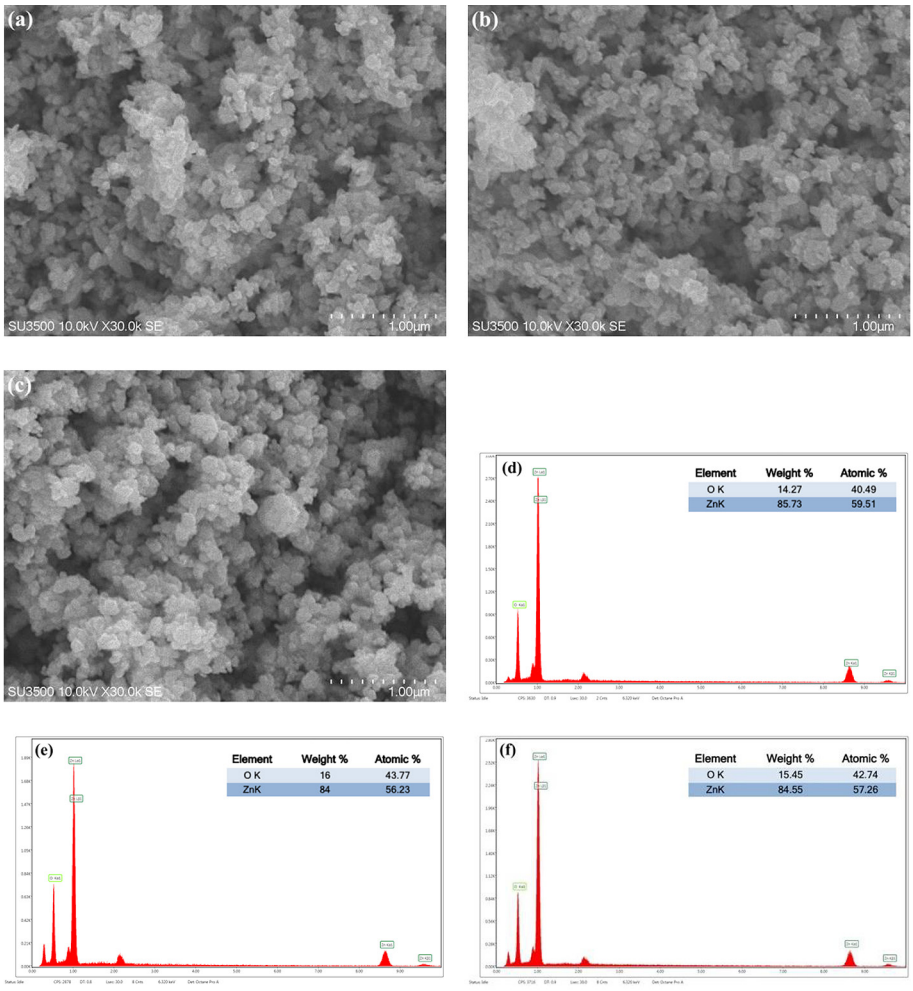

Figure 6. SEM image of Z1 (a), Z5(b), Z10 (c), and EDS spectra of Z1 (d), Z5 (e), Z10 (f)

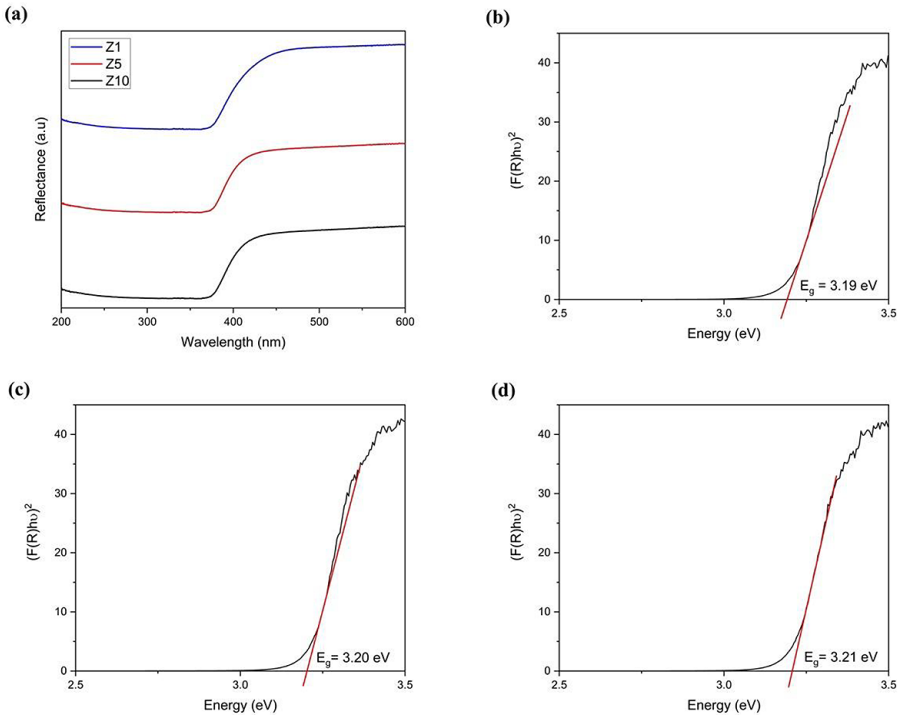

Figure 7. UV-DRS spectra of ZnO nanoparticles (a), Kubelka-Munk Plot of Z1 (b), Z5 (c), and Z10 (d)

$$F(R) = \frac{(1-R)^2}{2R} \quad (2)$$

where: R is the reflectance value and $F(R)$ is the equivalent to the absorption coefficient.

Figure 7b–7d depicts the Kubelka-Munk plots of the synthesized nanoparticles, $(F(R)h\nu)^2$ as a function of photon energy. The higher extract concentration was followed by the slightly increased band gap values as the crystallite size decrease (Z1=3.19 eV, Z5=3.20 eV, Z10=3.21 eV). The quantum confinement effect is responsible for the increase band gap value (Anbuvannan et al., 2015). These calculated band gap values had decreased, smaller than the bulk ZnO band gap energy. The ZnO nanoparticles capacity to absorb UV light improves and could possibly expand to the visible-light range if the band gap energy decreases. The increase in absorption efficiency is related to the enhanced performance of ZnO nanoparticles in photocatalytic activity. Therefore, ZnO nanoparticles demonstrate better performance in photocatalytic activity (Aldeen et al., 2022).

CONCLUSIONS

This research successfully synthesized ZnO nanoparticles utilizing biosynthesis method with *Indigofera tinctoria* leaf extract in methanol. The findings show that the phytochemical compounds in the extract act as bioreductor and the extract concentration affects the crystallite size and band gap energy of the nanoparticles. The crystallite size decreased as the extract concentration increased, while the band gap broadened. The decrease in crystallite size and increase in band gap indicate that the extract concentration has a considerable effect on the physical and optical properties of nanoparticles. This study supports the development of eco-friendly nanomaterials for the application in photocatalysts, sensors, pharmaceutical, and cosmetic industries. In addition, further study can be focused on optimizing synthesis conditions to improve production efficiency as well as direct application in various fields, including antimicrobial, waste treatment, and optoelectronic device development.

Acknowledgements

The authors would like to thank the Indonesia Endowment Funds for Education (LPDP) and the Center for Education Financial Services (PUSLAPDIK) (Grant Number: 0467/J5.2.3./BPI.06/10/2021) for the financial support of this work.

REFERENCES

1. Abbas, M., Buntinx, M., Deferme, W. & Peeters, R. (2019). (Bio)polymer/ZnO nanocomposites for packaging applications: A review of gas barrier and mechanical properties. *Nanomaterials*, *9*(10), 1–14. https://doi.org/10.3390/nano9101494
2. Abomuti, M. A., Danish, E. Y., Firoz, A., Hasan, N. & Malik, M. A. (2021). Green synthesis of zinc oxide nanoparticles using salvia officinalis leaf extract and their photocatalytic and antifungal activities. *Biology*, *10*(11), 1–26. https://doi.org/10.3390/biology10111075
3. Adam, F., Himawan, A., Aswad, M., Ilyas, S., Heryanto, Anugrah, M. A. & Tahir, D. (2021). Green synthesis of zinc oxide nanoparticles using Moringa oleifera l. water extract and its photocatalytic evaluation. *Journal of Physics: Conference Series*, *1763*(1), 1–8. https://doi.org/10.1088/1742-6596/1763/1/012002
4. Alamdari, S., Ghamsari, M. S., Lee, C., Han, W., Park, H., Tafreshi, M. J. & Afarideh, H. (2020). Preparation and Characterization of Zinc Oxide Nanoparticles Using Leaf Extract of Sambucus ebulus. *Applied Sciences*, *10*(3620), 1–19. doi:10.3390/app10103620
5. Aldeen, T. S., Ahmed Mohamed, H. E. & Maaza, M. (2022). ZnO nanoparticles prepared via a green synthesis approach: Physical properties, photocatalytic and antibacterial activity. *Journal of Physics and Chemistry of Solids*, *160*. https://doi.org/10.1016/j.jpcs.2021.110313
6. Alshehri, A. A. & Malik, M. A. (2019). Biogenic fabrication of ZnO nanoparticles using Trigonella foenum-graecum (Fenugreek) for proficient photocatalytic degradation of methylene blue under UV irradiation. *Journal of Materials Science: Materials in Electronics*, *30*(17). https://doi.org/10.1007/s10854-019-01985-8
7. Alyamani, A. A., Albukhaty, S., Aloufi, S., Almalki, F. A., Al-Karagoly, H. & Sulaiman, G. M. (2021). Green fabrication of zinc oxide nanoparticles using phlomis leaf extract: Characterization and in vitro evaluation of cytotoxicity and antibacterial properties. *Molecules*, *26*(20). https://doi.org/10.3390/molecules26206140
8. Anbuvannan, M., Ramesh, M., Viruthagiri, G., Shanmugam, N. & Kannadasan, N. (2015). Anisochilus carnosus leaf extract mediated synthesis of zinc oxide nanoparticles for antibacterial and photocatalytic activities. *Materials Science in Semiconductor Processing*, *39*. https://doi.org/10.1016/j.mssp.2015.06.005

9. Ashour, M., Mansour, A. T., Abdelwahab, A. M. & Alprol, A. E. (2023). Metal oxide nanoparticles' green synthesis by plants: prospects in phyto- and bioremediation and photocatalytic degradation of organic pollutants. *Processes 11*(12). https://doi.org/10.3390/pr11123356
10. Chandrakala, V., Aruna, V. & Angajala, G. (2022). Review on metal nanoparticles as nanocarriers: current challenges and perspectives in drug delivery systems. In *Emergent Materials*. https://doi.org/10.1007/s42247-021-00335-x
11. Chithiga, A. & Manimegalai, K. (2023). Biosynthesis of zinc oxide nanoparticles using Indigofera tinctoria and their efficacy against dengue vector, Aedes aegypti (Diptera: Culicidae). *Experimental Parasitology*, *249*. https://doi.org/10.1016/j.exppara.2023.108513
12. Dappula, S. S., Kandrakonda, Y. R., Shaik, J. B., Mothukuru, S. L., Lebaka, V. R., Mannarapu, M. & Amooru, G. D. (2023). Biosynthesis of zinc oxide nanoparticles using aqueous extract of Andrographis alata: Characterization, optimization and assessment of their antibacterial, antioxidant, antidiabetic and anti-Alzheimer's properties. *Journal of Molecular Structure*, *1273*. https://doi.org/10.1016/j.molstruc.2022.134264
13. Fadhila, F. R., Umar, A., Chandren, S., Apriandanu, D. O. B. & Yulizar, Y. (2024). Biosynthesis of $CoCr_2O_4$/ZnO nanocomposites using Basella alba L. leaves extracts with enhanced photocatalytic degradation of malachite green in aqueous media. *Chemosphere*, *352*. https://doi.org/10.1016/j.chemosphere.2024.141215
14. Faisal, S., Jan, H., Shah, S. A., Shah, S., Khan, A., Akbar, M. T., Rizwan, M., Jan, F., Wajidullah, Akhtar, N., Khattak, A. & Syed, S. (2021). Green synthesis of zinc oxide (ZnO) nanoparticles using aqueous fruit extracts of *Myristica fragrans*: Their characterizations and biological and environmental applications. *ACS Omega*, *6*(14). https://doi.org/10.1021/acsomega.1c00310
15. Fu, L. & Fu, Z. (2015). Plectranthus amboinicus leaf extract-assisted biosynthesis of ZnO nanoparticles and their photocatalytic activity. *Ceramics International*, *41*(2). https://doi.org/10.1016/j.ceramint.2014.10.069
16. Geetha, M. S., Nagabhushana, H. & Shivananjaiah, H. N. (2016). Green mediated synthesis and characterization of ZnO nanoparticles using Euphorbia Jatropa latex as reducing agent. *Journal of Science: Advanced Materials and Devices*, *1*(3). https://doi.org/10.1016/j.jsamd.2016.06.015
17. Ho, M. K., Chiu, H. H., Hsu, T. E., Chethan, B., Yu, S. L., Jheng, C. Y., Chin, C. E., Selvam, R., V, J. A., Cheng, C. L., Nagabhushana, H., Manjunatha, K. & Wu, S. Y. (2024). Advancing humidity sensing and magnetocaloric properties of spinel structural $CoCr_2O_4$ nanoparticles achieved via innovative bismuth doping by combustion synthesis. *Materials Today Chemistry*, *35*. https://doi.org/10.1016/j.mtchem.2024.101907
18. Isnaeni, I. N., Indriyati, Dedi, Sumiarsa, D. & Primadona, I. (2021). Green synthesis of different TiO2 nanoparticle phases using mango-peel extract. *Materials Letters*, *294*, 1–5. https://doi.org/10.1016/j.matlet.2021.129792
19. Joghee, S., Ganeshan, P., Vincent, A. & Hong, S. I. (2019). Ecofriendly biosynthesis of zinc oxide and magnesium oxide particles from medicinal plant *Pisonia grandis* R.Br. Leaf extract and their antimicrobial activity. *BioNanoScience*, *9*(1). https://doi.org/10.1007/s12668-018-0573-9
20. Kaningini, A. G., Azizi, S., Sintwa, N., Mokalane, K., Mohale, K. C., Mudau, F. N. & Maaza, M. (2022). Effect of optimized precursor concentration, temperature, and doping on optical properties of ZnO nanoparticles synthesized via a green route using bush tea (*Athrixia phylicoides* DC.) leaf extracts. *ACS Omega*, *7*(36). https://doi.org/10.1021/acsomega.2c00530
21. Kumara Swamy, M., Sudipta, K. M., Jayanta, K. & Balasubramanya, S. (2015). The green synthesis, characterization, and evaluation of the biological activities of silver nanoparticles synthesized from Leptadenia reticulata leaf extract. *Applied Nanoscience (Switzerland)*, *5*(1). https://doi.org/10.1007/s13204-014-0293-6
22. Lusvardi, G., Barani, C., Giubertoni, F. & Paganelli, G. (2017). Synthesis and characterization of TiO_2 nanoparticles for the reduction of water pollutants. *Materials*, *10*(10), 1–11. https://doi.org/10.3390/ma10101208
23. Marín, R. M., de Oca Porto, R. M., Herrera Paredes, M. E., Alarcón, A. B., Balmaseda, I. H., Soto del Valle, R. M., Lopes, M. T. P. & Guerra, I. R. (2018). GC/MS analysis and bioactive properties of extracts obtained from Clusia minor L. Leaves. *Journal of the Mexican Chemical Society*, *62*(4). https://doi.org/10.29356/jmcs.v62i4.544
24. Marouzi, S., Sabouri, Z. & Darroudi, M. (2021). Greener synthesis and medical applications of metal oxide nanoparticles. *Ceramics International*, *47*(14). https://doi.org/10.1016/j.ceramint.2021.03.301
25. Momoh, J. O., Kumar, S., Olaleye, O. N., Adekunle, O. M. & Aiyelero, T. S. (2024). Green synthesis of characterized bio-functionalized ZnO nanoparticles from *Terminalia catappa* (Almond) methanol leaf extract and their potential antioxidant and antibacterial properties. *Tropical Journal of Natural Product Research*, *8*(11), 9296–9309. https://doi.org/10.26538/tjnpr/v8i11.45
26. Mthana, M. S., Mthiyane, D. M. N., Onwudiwe,

D. C. & Singh, M. (2022). Biosynthesis of ZnO nanoparticles using capsicum chinense fruit extract and their in vitro cytotoxicity and antioxidant assay. *Applied Sciences (Switzerland)*, *12*(9), 1–13. https://doi.org/10.3390/app12094451

27. Mushtaq, W., Ishtiaq, M., Maqbool, M., Mazhar, M. W., Casini, R., Abd-ElGawad, A. M. & Elansary, H. O. (2023). Green synthesis of zinc oxide nanoparticles using viscum album extracts: unveiling bioactive compounds, antibacterial potential, and antioxidant activities. *Plants*, *12*(11). https://doi.org/10.3390/plants12112130
28. Mishra D. N., Gomare K. S., & Sheelwant V. S. (2020). GC-MS Analysis and phytochemical screening of *Indigofera tinctoria* (Linn.) leaf extract characterizing its medicinal use. *International Journal of Ayurvedic Medicine*, *11*(2), 289–299. https://doi.org/10.47552/ijam.v11i2.1540
29. Nabi, G., Majid, A., Riaz, A., Alharbi, T., Arshad Kamran, M. & Al-Habardi, M. (2021). Green synthesis of spherical TiO_2 nanoparticles using *Citrus limetta* extract: Excellent photocatalytic water decontamination agent for RhB dye. *Inorganic Chemistry Communications*, *129*, 1–8. https://doi.org/10.1016/j.inoche.2021.108618
30. Nadeem, M., Tungmunnithum, D., Hano, C., Abbasi, B. H., Hashmi, S. S., Ahmad, W. & Zahir, A. (2018). The current trends in the green syntheses of titanium oxide nanoparticles and their applications. *Green Chemistry Letters and Reviews*, *11*(4), 492–502. https://doi.org/10.1080/17518253.2018.1538430
31. Nath, M. R., Ahmed, A. N., Gafur, M. A., Miah, M. Y. & Bhattacharjee, S. (2018). ZnO nanoparticles preparation from spent zinc–carbon dry cell batteries: studies on structural, morphological and optical properties. *Journal of Asian Ceramic Societies*, *6*(3). https://doi.org/10.1080/21870764.2018.1507610
32. Nunes, V. F., Maia, P. H. F., Almeida, A. F. L. & Freire, F. N. A. (2024). Surface properties of Al_2O_3:ZnO thin films growth on FTO for photovoltaic application. *Next Materials*, *2*. https://doi.org/10.1016/j.nxmate.2023.100069
33. Obeizi, Z., Benbouzid, H., Ouchenane, S., Yılmaz, D., Culha, M. & Bououdina, M. (2020). Biosynthesis of zinc oxide nanoparticles from essential oil of *Eucalyptus globulus* with antimicrobial and anti-biofilm activities. *Materials Today Communications*, *25*, 1–10. https://doi.org/10.1016/j.mtcomm.2020.101553
34. Parmar, M. & Sanyal, M. (2022). Extensive study on plant mediated green synthesis of metal nanoparticles and their application for degradation of cationic and anionic dyes. In *Environmental Nanotechnology, Monitoring and Management*,17, 1–18. https://doi.org/10.1016/j.enmm.2021.100624
35. Quevedo-Robles, R. V., Vilchis-Nestor, A. R. & Luque, P. A. (2022). Study of optical and morphological properties of nanoparticles semiconductors of zinc oxide synthesized using Mimosa tenuiflora extract for photodegradation of methyl orange. *Optical Materials*, *128*, 1–9. https://doi.org/10.1016/j.optmat.2022.112450
36. Rafeeq, C. M., Paul, E., Vidya Saagar, E. & Manzur Ali, P. P. (2021). Mycosynthesis of zinc oxide nanoparticles using *Pleurotus floridanus* and optimization of process parameters. *Ceramics International*, *47*(9). https://doi.org/10.1016/j.ceramint.2021.01.091
37. Rajan, A. K. & Cindrella, L. (2019). Studies on new natural dye sensitizers from Indigofera tinctoria in dye-sensitized solar cells. *Optical Materials*, *88*, 39–47. https://doi.org/10.1016/j.optmat.2018.11.016
38. Ramesh, M., Anbuvannan, M. & Viruthagiri, G. (2015). Green synthesis of ZnO nanoparticles using Solanum nigrum leaf extract and their antibacterial activity. *Spectrochimica Acta - Part A: Molecular and Biomolecular Spectroscopy*, *136*(PB). https://doi.org/10.1016/j.saa.2014.09.105
39. Rilda, Y., Arief, S., Agustien, A., Yerizel, E., Pardi, H. & Sofyan, N. (2022). Growth inhibition of bacterial pathogens by photo-catalyst process of nano-alloys FeCuNi doped TiO_2 under ultraviolet irradiation. *Heliyon*, *8*(9). https://doi.org/10.1016/j.heliyon.2022.e10611
40. Sadiq, H., Sher, F., Sehar, S., Lima, E. C., Zhang, S., Iqbal, H. M. N., Zafar, F. & Nuhanović, M. (2021). Green synthesis of ZnO nanoparticles from *Syzygium cumini* leaves extract with robust photocatalysis applications. *Journal of Molecular Liquids*, *335*, 1–9. https://doi.org/10.1016/j.molliq.2021.116567
41. Shaikhaldein, H. O., Al-qurainy, F., Khan, S., Nadeem, M., Tarroum, M., Salih, A. M., Gaafar, A. R. Z., Alshameri, A., Alansi, S., Alenezi, N. A. & Alfarraj, N. S. (2021). Biosynthesis and characterization of ZnO nanoparticles using ochradenus arabicus and their effect on growth and antioxidant systems of maerua oblongifolia. *Plants*, *10*(9), 1–14. https://doi.org/10.3390/plants10091808
42. Sheik Mydeen, S., Raj Kumar, R., Kottaisamy, M. & Vasantha, V. S. (2020). Biosynthesis of ZnO nanoparticles through extract from Prosopis juliflora plant leaf: Antibacterial activities and a new approach by rust-induced photocatalysis. *Journal of Saudi Chemical Society*, *24*(5), 393–406. https://doi.org/10.1016/j.jscs.2020.03.003
43. Srinivasan, S., Wankhar, W., Rathinasamy, S. & Rajan, R. (2015). Larvicidal potential of *Indigofera tinctoria* (Fabaceae) on dengue vector (*Aedes aegypti*) and its antimicrobial activity against clinical isolates. *Asian Journal of Pharmaceutical and Clinical Research*, *8*(3).
44. Swamy M. M., Surendra B. S., Mallikarjunaswamy C., Pramila S., & Rekha N. D. (2021). Bio-mediated

synthesis of ZnO nanoparticles using *Lantana camara* flower extract: Its characterizations, photocatalytic, electrochemical and anti-inflammatory applications. *Environmental Nanotechnology, Monitoring and Management*, *15*. https://doi.org/10.1016/j.enmm.2021.100442

45. Prasad T. S., & Joseph, A.R (2024). Synthesis, characterization, and effective removal of dye pollutants from water bodies using a new ZnO nanocomposite. *Journal of the Indian Chemical Society*, *101*(8). https://doi.org/10.1016/j.jics.2024.101183
46. Tahya, C. Y. & Karnelasatri, K. (2021). Gas Chromatography-Mass Spectrometry Analysis and α-Glucosidase Inhibitory Activity of n-Hexane Extract of Bilajang Bulu (Merremia Vitifolia) Leaves. *Walisongo Journal of Chemistry*, *4*(2). https://doi.org/10.21580/wjc.v4i2.9427
47. Thema, F. T., Manikandan, E., Dhlamini, M. S. & Maaza, M. (2015). Green synthesis of ZnO nanoparticles via Agathosma betulina natural extract. *Materials Letters*, *161*. https://doi.org/10.1016/j.matlet.2015.08.052
48. Uribe-López, M. C., Hidalgo-López, M. C., López-González, R., Frías-Márquez, D. M., Núñez-Nogueira, G., Hernández-Castillo, D. & Alvarez-Lemus, M. A. (2021). Photocatalytic activity of ZnO nanoparticles and the role of the synthesis method on their physical and chemical properties. *Journal of Photochemistry and Photobiology A: Chemistry*, *404*. https://doi.org/10.1016/j.jphotochem.2020.112866
49. Vandamar Poonguzhali, R., Ranjith Kumar, E., Sumithra, M. G., Arunadevi, N., Rahale, C. S., Munshi, A. M., Mersal, G. A. M. & El-Metwaly, N. M. (2021). Natural citric acid (lemon juice) assisted synthesis of ZnO nanostructures: Evaluation of phase composition, morphology, optical and thermal properties. *Ceramics International*, *47*(16). https://doi.org/10.1016/j.ceramint.2021.05.024
50. Vijayan, R., Joseph, S. & Mathew, B. (2018). Indigofera tinctoria leaf extract mediated green synthesis of silver and gold nanoparticles and assessment of their anticancer, antimicrobial, antioxidant and catalytic properties. *Artificial Cells, Nanomedicine and Biotechnology*, *46*(4), 861–871. https://doi.org/10.1080/21691401.2017.1345930
51. Xie, H., Lv, X., Mo, Z., Gong, J., Gao, X., Li, Z., Wu, J. & Shen, J. (2024). Tailoring the cryogenic magnetism and magnetocaloric effect from Zr substitution in $EuTiO_3$ perovskite. *Journal of Materials Science and Technology*, *193*. https://doi.org/10.1016/j.jmst.2024.01.041
52. Yasser, M., Rafi, M., Wahyuni, W. T., Widiyanti, S. E. & Asfar, A. M. I. A. (2020). Total phenolic content and antioxidant activities of buni fruit (*Antidesma bunius* L.) in moncongloe maros district extracted using ultrasound-assisted extraction. *Rasayan Journal of Chemistry*, *13*(1). https://doi.org/10.31788/RJC.2020.1315584